

Manuscript Number:

Title: Non-destructive evaluation of stiffness moduli of cemented soils out of resonant frequency

Article Type: Technical Paper

Keywords: cement; clay; small-strain stiffness; resonant frequency; laboratory testing.

Corresponding Author: Dr. Ramiro Daniel Verastegui Flores,

Corresponding Author's Institution: Université catholique de Louvain

First Author: Ramiro Daniel Verastegui Flores

Order of Authors: Ramiro Daniel Verastegui Flores; Gemmina Di Emidio; Adam Bezuijen; Joachim Vanwalleghem; Mathias Kersemans

**Abstract:** The objective of this research was to determine small-strain stiffness of cement-treated clay by means of the free-free resonant column test. In the test, a cylindrical soil specimen is laid on top of a soft foam layer to simulate fully free boundary conditions. Next an accelerometer is put in contact with one end of the specimen to measure vibrations while the other end is impacted with a light hammer. Knowing the density, dimensions and fundamental frequency of vibration, the small-strain moduli can be evaluated. Factors that can affect the outcome, include the actual boundary conditions of the sample, the interference of the accelerometer on the vibrational response of the sample and the shape of the sample given by the ratio diameter to length. In order to verify the reliability of the measurements, the free-free resonant column test was compared with a more robust technique like the laser doppler vibrometer. Furthermore the impact of the samples shape was investigated through numerical modal analysis from which also correction factors were proposed to improve the reliability of the interpretations.

# Non-destructive evaluation of stiffness moduli of cemented soil out of resonant frequency

R.D. Verástegui Flores<sup>a,b,\*</sup>, G. Di Emidio<sup>b</sup>, A. Bezuijen<sup>b</sup>, J. Vanwalleghem<sup>c</sup>,  
M. Kersemans<sup>c</sup>

<sup>a</sup>*iMMC, Université catholique de Louvain, Belgium*

<sup>b</sup>*Laboratory of Geotechnics, Ghent University, Belgium*

<sup>c</sup>*Department of Material Science and Engineering, Ghent University, Belgium*

---

## Abstract

The objective of this research was to determine small-strain stiffness of cement-treated clay by means of the free-free resonant column test. In the test, a cylindrical soil specimen is laid on top of a soft foam layer to simulate fully free boundary conditions. Next an accelerometer is put in contact with one end of the specimen to measure vibrations while the other end is impacted with a light hammer. Knowing the density, dimensions and fundamental frequency of vibration, the small-strain moduli can be evaluated. Factors that can affect the outcome, include the actual boundary conditions of the sample, the interference of the accelerometer on the vibrational response of the sample and the shape of the sample given by the ratio diameter to length. In order to verify the reliability of the measurements, the free-free resonant column test was compared with a more robust technique like the laser doppler vibrometer. Furthermore the impact of the samples shape was investigated through numerical modal analysis from which also correction factors were

---

\*Corresponding author

*Email address:* ramiro.verastegui@uclouvain.be (R.D. Verástegui Flores )

proposed to improve the reliability of the interpretations.

*Keywords:* cement, clay, stiffness, resonant frequency, laboratory testing

---

## 1. Introduction

The stress-strain behaviour of soil is complex and non-linear. Therefore, the Young's modulus ( $E$ ) and shear modulus ( $G$ ) of soil are not constants but they may significantly change with strain level. At small strains, the stiffness is relatively large while at strains close to failure the stiffness is small. However, it has been observed that behaviour is sufficiently constant and linear below a strain level of about 0.001% (Clayton, 2011). It is in such range that small-strain moduli ( $E_0$  and  $G_0$ ) are defined. Small-strain moduli may be estimated from local strain gauges but the use of wave-propagation based methods has gained popularity due to its relative simplicity. The present paper focuses on the determination of  $E_0$  and  $G_0$  of cement-treated soil.

In general, small-strain stiffness is governed by a number of factors such as stress history, void ratio, soil fabric, and the interparticle contact stiffness, which will depend upon particle mineralogy, angularity and roughness, and effective stress. The small-strain stiffness is an important parameter for a variety of geotechnical design applications including small-strain dynamic analyses such as those to predict soil behaviour or soil-structure interaction during earthquake, explosions or machine or traffic vibration. Small-strain stiffness may also be used as an indirect indication of other soil parameters, as it in many cases correlates well to other soil properties. For example, when studying the hardening process of cement-treated soil, an increase of stiffness

can be expected with increasing interparticle cementation and compressive strength.

The laboratory determination of small-strain stiffness is usually carried out through direct methods such as the bender/extender elements (Åhnberg and Holmen, 2008; Verástegui Flores et al., 2010; Seng and Tanaka, 2011; Åhnberg and Holmen, 2011). But, there are also indirect methods for measuring small-strain stiffness such as the free-free resonant column test (Nazarian et al., 2005; Rydén, 2009; Åhnberg and Holmen, 2011; Toohey and Mooney, 2012; Schaeffer et al., 2013; Guimond-Barret et al., 2013)

The free-free resonant column (FFR) is a simple test to execute and it could be a good alternative to bender/extender element testing of cemented soil. In FFR testing, a cylindrical specimen is allowed to vibrate at its fundamental frequency and the stiffness is evaluated out of the measured frequency, density and length of the specimen through a straightforward formula based on theories of one-dimensional wave propagation in an elastic rod. However, the interpretation of stiffness out of FFR results might be affected by uncertainties related to the boundary conditions (which in the laboratory are not perfectly free) and also by the length-to-diameter ratio of the specimen (Åhnberg and Holmen, 2011; Schaeffer et al., 2013).

The objective of this study is to address these uncertainties of FFR testing. The correctness of the measured fundamental frequencies out of FFR testing is evaluated and compared with a reliable reference obtained with a laser doppler vibrometer. Whereas, the impact of the specimen shape is studied numerically through modal analysis in Abaqus. Experiments were carried out on cylindrical specimens of different dimensions consisting of

1  
2  
3  
4  
5  
6  
7  
8  
9  
10 cement-treated kaolin clay.  
11

## 12 2. Materials and sample preparation 13 14

15 The cement-treated clay used in this research consists of kaolin clay mixed  
16  
17 with blast-furnace slag cement of the type CEM III/B (EN 197-1, 2011) and  
18  
19 demonised water.  
20

21 A commercial processed kaolin Rotoclay HB (Goonvean, St. Austell,  
22  
23 UK) was used in this investigation. The clay was available as a dry powder.  
24  
25 Table 1 summarises some properties of this material. The blast-furnace slag  
26  
27 cement used in the experiments, CEM III/B 42.5 N LH/SR LA, consists of  
28  
29 approximately 70% of ground granulated blast furnace slag, 26% of Portland  
30  
31 clincker and 4% of gypsum. It shows a minimal normalised mortar strength  
32  
33 at 28 days, of 42.5 N/mm<sup>2</sup>. Moreover, this cement features improved sulphate  
34  
35 resistance, low hydration heat and low alkali content.  
36

37 Deionised water was used for the admixture of soil and cement. The  
38  
39 electrical conductivity ( $EC$ ) and pH of the deionized water was  $EC < 4$   
40  
41  $\mu\text{S}/\text{cm}$  and  $\text{pH} \approx 7$  respectively.  
42

43 The clay and cement were initially mixed dry in a dough mixer for about  
44  
45 2 minutes until a homogeneous cement distribution was observed. The ce-  
46  
47 ment dosage was fixed to 10% (in dry mass). Next, deionised water was  
48  
49 poured in the mixing bowl to achieve a clay water content of twice its liquid  
50  
51 limit in order to obtain a liquid consistency to simplify the preparation of  
52  
53 homogeneous specimens of similar properties. The slurry of clay and cement  
54  
55 was thoroughly mixed for another 7 minutes approximately. Then, the fresh  
56  
57 clay-cement mix was poured into stainless steel cylindrical moulds of differ-  
58  
59  
60  
61  
62  
63  
64  
65

ent dimensions. The cylindrical moulds were lightly vibrated while filling them with the fresh mix to remove any trapped air bubbles. The bottom and top ends of the moulds were sealed with kitchen foil to prevent moisture loss. Then, the samples were allowed to cure inside the moulds for one week in a conditioned room at about 20°C. After that period, the specimens were trimmed with a spatula to flatten the top and bottom ends and they were carefully extruded out of the moulds. Finally they were stored under water for further testing.

Specimens with diameter ( $D$ ) and length ( $L$ ) of  $D = 38\text{mm}$  &  $L = 85\text{mm}$  ( $D/L = 0.44$ ),  $D = 50\text{mm}$  &  $L = 100\text{mm}$  ( $D/L = 0.5$ ) and  $D = 70\text{mm}$  &  $L = 130\text{mm}$  ( $D/L = 0.54$ ) were produced.

### 3. Methods

#### 3.1. Free-free resonant column test

The free-free resonant column test (FFR) is an attractive alternative (due to its simplicity) to measure the small-strain Young's modulus and shear modulus of (unconfined) cemented or cohesive soil in the laboratory (Nazarian et al., 2005; Rydén, 2009; Åhnberg and Holmen, 2011; Toohey and Mooney, 2012; Schaeffer et al., 2013; Guimond-Barret et al., 2013). From 1D wave propagation theory of elastic rods, it is known that the fundamental frequency of vibration of a specimen is determined by its stiffness, so these two parameters can be correlated through a simple formula, as long as the specimen fits in the definition of rod (e.g.  $L \gg D$ ).

Figure 1 illustrates the FFR testing setup used in this study. Here, the cylindrical soil samples are laid horizontally on top of a 30mm thick soft

foam to simulate fully free boundary conditions. A small hammer is used to excite the specimens. The hammer should have most of its mass concentrated at the point of impact and it should have enough mass to induce a measurable mechanical vibration, but not too much as to displace or damage the specimen. The hammer used in this research consists of a glass bead of about 4mm in diameter glued to the end of a flexible 10-cm long plastic rod. The vibrational response of the specimen was captured with a compact-size accelerometer type PCB A353B68 with a frequency range up to 10 kHz. The accelerometer was put in contact with a specimen at its anti-nodes with the help of a support arm. Fig. 1a shows the configuration of accelerometer and hammer impact for measuring the fundamental frequency of vibration in the longitudinal (axial) direction; while, Fig. 1b illustrates the configuration for measuring the transversal fundamental frequency.

Figure 2 shows an example of determination of the fundamental frequency of a specimen. A recorded time-domain vibration signal is illustrated in Fig. 2a. Frequency domain analysis performed on this signal through the fast Fourier transform is illustrated in Fig. 2b. A clear dominant frequency can always be identified; moreover, the frequency-domain response to consecutive hammer impacts is very repeatable.

The interpretation of  $E_0$  and  $G_0$  is done based on the following formulas, valid for isotropic elastic rods.

$$E_0 = \rho v_p^2 = \rho (2 L f_L)^2 \quad (1)$$

$$G_0 = \rho v_s^2 = \rho (2 L f_T)^2 \quad (2)$$

where  $\rho$  is the bulk density,  $L$  is the length of the rod,  $f_L$  is the longitudinal

1  
2  
3  
4  
5  
6  
7  
8  
9  
10  
11  
12  
13  
14  
15  
16  
17  
18  
19  
20  
21  
22  
23  
24  
25  
26  
27  
28  
29  
30  
31  
32  
33  
34  
35  
36  
37  
38  
39  
40  
41  
42  
43  
44  
45  
46  
47  
48  
49  
50  
51  
52  
53  
54  
55  
56  
57  
58  
59  
60  
61  
62  
63  
64  
65

119 fundamental frequency,  $f_T$  is the torsional fundamental frequency,  $v_p$  is the  
120 compressive wave velocity and  $v_s$  is the shear wave velocity. Both wave  
121 velocities are evaluated assuming that the wavelength ( $\lambda$ ) of the vibrating  
122 rod is equal to twice its length  $\lambda = 2 L$ . This assumption is acceptable for  
123 free-free specimens having  $D/L \leq 0.5$  (ASTM C 215, 1999; Rydén, 2009).

124 It remains difficult to measure the torsional fundamental frequency of  
125 cylindrical specimens with a basic FFR setup. Therefore, many authors as-  
126 sume that  $f_T \approx f_{Tr}$  for  $D/L \leq 0.5$  (e.g. Åhnberg and Holmen, 2011; Toohey  
127 and Mooney, 2012; Guimond-Barret et al., 2013). The validity of this as-  
128 sumption will be discussed in the next section by means of numerical modal  
129 analysis of cylindrical specimens of different dimensions.

### 3.2. *Laser doppler vibrometer test*

131 The laser doppler vibrometer (LDV) has been applied for modal and vi-  
132 brational analysis in different research areas: including mechanical engineer-  
133 ing, to biomedics, archaeology, food science and civil engineering (Castellini  
134 et al., 2006). LDV features extended measurement capabilities with respect  
135 to traditional vibration sensors (e.g. accelerometers) as it allows for contact-  
136 less measurement (avoiding transducer mass loading effects) with reduced  
137 testing time and increased performance (Muramatsu et al., 1997; De Pauw  
138 et al., 2013).

139 The resonance frequencies of a specimen are assessed by measuring its  
140 vibration response to an input excitation. In this study the samples were  
141 excited through acoustic excitation from a 60 W rms loudspeaker (type:  
142 SP-W65-SONO woofer). The sample was excited with white noise from  
143 which the frequency content was concentrated near the sample's resonance



frequency estimated from FFR testing. The velocity response was measured with a laser Doppler vibrometer (LDV) system consisting of a vibrometer controller Polytec OFV-5000 with the corresponding velocity decoder VD-06 and OFV-534 sensor head. The laser beam was pointed on the anti-nodal position of the vibration mode of the specimen and the samples reflectivity was improved by spraying micro glass spheres on the measuring point. Data acquisition was done through a National Instruments NI9215 module with a sampling frequency of 8192 Hz. Finally, the resonance frequency was evaluated from conversion of the time-domain signal to the frequency domain with the Fast Fourier algorithm.

Moreover, in order to improve the quality of vibration response measurements, the samples were suspended with nylon wires (Fig. 3) to mimic free vibration conditions and to minimise the effect of perturbing external factors on the sample's resonance frequencies. The sample is positioned with its axis perpendicular to the laser beam for measuring the transversal fundamental frequency and with its axis parallel to the laser beam for measuring the longitudinal fundamental frequency.

## 4. Results and discussion

### 4.1. Free-free resonant column vs. Laser Doppler Vibrometer

The testing program consisted of continuous monitoring of  $E_0$  and  $G_0$  increase due to cement hydration of all three groups of specimens ( $D/L = 0.44$ ,  $D/L = 0.50$ ,  $D/L = 0.54$ ) by means of FFR tests. In parallel, LDV measurements were also carried out on each sample type at specific time steps (28 days and 90 days).

LDV tests were carried out here to compare and evaluate the outcome of FFR tests. As suggested in the literature (e.g. Muramatsu et al., 1997; De Pauw et al., 2013), LDV is a better performing technique to measure the vibrational response of samples. Figure 4 compares the measured longitudinal and transversal frequencies out of both methods for all samples. Excellent agreement can be observed which confirms that the results obtained through the FFR technique are reliable. Moreover, it can be concluded that the FFR testing setup used in this study shows negligible errors due to the imperfect free-free boundary conditions and the transducer mass loading effects.

#### 4.2. Effect of $D/L$ on the vibrational response in FFR testing

Results of FFR testing on the three series of specimens with different  $D/L$  ratios are summarised in figure 5. As expected, the calculated small-strain stiffness moduli increase with time due to cement hydration. For clarity, these calculated stiffness values out of the measured  $f_L^*$  and  $f_{Tr}^*$  (assuming  $f_T^* \approx f_{Tr}^*$ ) will be denoted as  $E_0^*$  and  $G_0^*$ .

The small-strain Young's modulus  $E_0^*$  seems unaffected by the shape ratio  $D/L$  as all results fall very close within a well-defined trend. However, that is not the case for the small-strain shear modulus  $G_0^*$  that is clearly affected by the ratio  $D/L$ .  $G_0^*$  is calculated based on Eq. 2 and the assumption  $f_T^* \approx f_{Tr}^*$ . For any given time step,  $G_0^*$  increases with increasing  $D/L$ . A significant spreading of  $G_0^*$  values is observed even for small changes of  $D/L$  around the recommended value of  $D/L = 0.5$ .

In order to evaluate the suitability and the limitations of the simple interpretation formulas (Eq. 1 and 2) of FFR testing, numerical modal analysis was carried out in a finite element program (Abaqus), where cylindrical

elastic specimens of different  $D/L$  ratios were modelled. Figure 6 shows the 3 fundamental vibration modes considered in this study: longitudinal, transversal and torsional vibrations.

Figure 7 summarises the outcome of fundamental frequency calculations vs.  $D/L$  for a hypothetical material with the following properties:  $E_0 = 400\text{MPa}$ , Poisson ratio  $\nu = 0.3$  and density  $\rho = 1400 \text{ kg/m}^3$ . The figure shows as well the back calculated values of  $f_L$  and  $f_T$  out of equations 1 and 2 respectively.

These results show that the fundamental longitudinal frequency  $f_L$  is only slightly affected by  $D/L$ . Equation 1 matches the modal-analysis outcome for the lower range of  $D/L$  values (sample shape approaching to a rod) as suggested by literature (e.g. ASTM C 215, 1999; Rydén, 2009).

The fundamental torsional frequency  $f_T$  out of modal analysis seems independent of  $D/L$  and it perfectly matches the back calculated frequency from equation 2. Whereas, the fundamental transversal frequency  $f_{Tr}$  is strongly affected by  $D/L$  and it only matches equation 2 at  $D/L \approx 0.5$ . These results suggest that care must be taken when assuming  $f_T = f_{Tr}$  for the evaluation of  $G_0$ , as small deviations from  $D/L \approx 0.5$  could lead to significant spreading of estimated  $G_0$  values.

In order to minimise errors of interpretation due to finite dimensions of cylindrical specimens, correction factors could be applied. Then, the correct value of  $f_L$  or  $f_T$  could be obtained through the following formulas:

$$f_L = \frac{f_L^*}{K_E} \quad (3)$$

$$f_T = \frac{f_{Tr}^*}{K_G} \quad (4)$$

where  $f_L^*$  and  $f_{Tr}^*$  are the measured fundamental longitudinal frequency and the measured fundamental transversal frequency; moreover,  $K_E$  and  $K_G$  are correction factors evaluated from modal analysis for different scenarios.  $K_E$  and  $K_G$  are given in table 2 and 3 respectively as functions of Poisson ratio  $\nu$ .

Substituting Eq. 3 and 4 into Eq. 1 and 2 respectively, the following small-strain stiffness interpretation formulas are obtained:

$$E_0 = \rho \frac{(2 L f_L^*)^2}{K_E^2} = \frac{E_0^*}{K_E^2} \quad (5)$$

$$G_0 = \rho \frac{(2 L f_{Tr}^*)^2}{K_G^2} = \frac{G_0^*}{K_G^2} \quad (6)$$

The correction factors  $K_E^2$  and  $K_G^2$  for the determination of small-strain stiffness are illustrated in figure 8. For the case of  $E_0$  (Fig. 8a), it appears that FFR testing could underestimate  $E_0$  by less than 5% for  $D/L \leq 0.5$ . On the other hand, figure 8b shows that the relationship between  $K_G^2$  and  $D/L$  is rather linear for  $0 < D/L < 0.6$  approximately, then the correction formula can be simplified to:

$$G_0 = \frac{\psi}{D/L} \rho (2 L f_{Tr}^*)^2 = \frac{\psi}{D/L} G_0^* \quad (7)$$

where  $\psi$  is the  $D/L$  ratio corresponding to  $K_G^2 = 1$ .  $\psi$  is a function of Poisson ratio ( $\nu$ ) and is given by:

$$\psi = 0.379 \nu^2 - 0.577 \nu + 0.657 \quad (8)$$

These correction formulas either for the frequency or the small-strain stiffness will allow to produce accurate estimations of  $E_0$  and  $G_0$  irrespective

of  $D/L$ . As an example, the data originally presented in figure 5 has been subjected to correction factors and the results are illustrated in figure 9. While  $E_0$  has only been minimally affected,  $G_0$  shows the most significant improvement as the data dispersion has disappeared and now all results follow the same trend.

## 5. Conclusions

The objective of this research was to address uncertainties of free-free-resonant column testing (FFR). The correctness of the measured fundamental frequencies out of FFR testing was evaluated by comparing it to a reliable reference obtained with a laser doppler vibrometer (LDV). Furthermore, the impact of the specimen shape ( $D/L$  ratio) on its vibrational response was studied numerically through modal analysis in Abaqus.

Excellent agreement could be observed between FFR and LDV frequency measurements and which confirms that the results obtained through the FFR technique are reliable. Moreover, it can be concluded that the FFR testing setup used in this study shows negligible errors due to the imperfect free-free boundary conditions and the transducer mass loading effects.

Results of numerical modal analysis of elastic cylindrical elements show that the fundamental longitudinal frequency is only slightly affected by  $D/L$ . The lower  $D/L$ , the better the match between modal analysis frequency and the stiffness interpretation formula which is based on 1D wave propagation along an elastic rod.

The fundamental torsional frequency  $f_T$  out of modal analysis seems independent of  $D/L$ . Whereas, the fundamental transversal frequency  $f_{Tr}$  is

strongly affected by  $D/L$  and it only matches the stiffness interpretation formula at  $D/L \approx 0.5$ . These results suggest that care must be taken when assuming  $f_T = f_{Tr}$  for the evaluation of  $G_0$ , as small deviations from  $D/L \approx 0.5$  could lead to significant spreading of estimated  $G_0$  values.

Based on numerical modal analysis a set of correction factors were proposed. They could allow to produce more accurate estimations of  $E_0$  and  $G_0$  irrespective of  $D/L$ .

## Acknowledgements

The authors would like to thank ir. Bert D'hondt for his contribution to the realisation of this work.

## References

## References

ASTM C 215, 1999. Standard test method for fundamental transverse, longitudinal and torsional resonant frequencies of concrete specimens, ASTM International.

ASTM D 854, 2010. Standard test methods for specific gravity of soil solids by water pycnometer, ASTM International.

ASTM D 4318, 2010. Standard test methods for liquid limit, plastic limit, and plasticity index of soils, ASTM International.

ASTM D 5890, 2011. Standard test method for swell index of clay mineral component of geosynthetic clay liners, ASTM International.

- 278 Åhnberg, H., Holmen, M., 2008. Laboratory determination of small-strain  
279 moduli in stabilised soils. *Proc. Deformational Characteristics of Geoma-*  
280 *terials*, IOS Press, 291-297.
- 281 Åhnberg, H., Holmen, M., 2011. Assessment of stabilised soil strength with  
282 geophysical methods. *Ground Improvement* 164(3), 109-116.
- 283 Castellini, P., Martarelli, M., Tomasini, E.P., 2006. Laser Doppler Vibrome-  
284 try: Development of advanced solutions answering to technology's needs.  
285 *Mechanical Systems and Signal Processing* 20(6), 1265-1285.
- 286 Clayton, C.R.I., 2011. Stiffness at small strain: research and practice.  
287 *Géotechnique* 61(1), 5-37.
- 288 De Pauw, B., Vanlanduit, S., Van Tichelen, K., Geernaert, T., Chah, K.,  
289 Berghmans, F., 2013. Benchmarking of deformation and vibration mea-  
290 surement techniques for nuclear fuel pins. *Measurement* 46, 3647-3653.
- 291 EN 197-1, 2011. Cement. Composition, specifications and conformity criteria  
292 for common cements. European Committee for Standardization.
- 293 Guimond-Barrett, A., Nauleau, E., Le Kouby, A., Pantet, A., Reiffsteck, P.,  
294 2013. Free-free resonance testing of in situ deep mixed soils. *Geotechnical*  
295 *Testing Journal* 36(2), 283-291.
- 296 Muramatsu, N., Sakurai, N., Wada, N., Yamamoto, R., Tanaka, K., Asakura,  
297 T., Ishikawa-Takano, Y., Nevins, D.J. 1997. Critical comparison of an ac-  
298 celerometer and a laser doppler vibrometer for measuring fruit firmness.  
299 *HortTech* 7, 434-438.

- 300 Nazarian, S., Yuan, D., Tandon, V., and Arellano, M., 2005. Quality man-  
 301 agement of flexible pavement layers by seismic methods. Research Report  
 302 0-1735-3, Center for Transportation Infrastructure Systems, The Univer-  
 303 sity of Texas at El Paso, El Paso, Texas.
- 304 Rydén, N., 2009. Determining the asphalt mastercurve from free-free reso-  
 305 nant testing on cylindrical samples. Proc. of the 7<sup>th</sup> Int. Symp. on Non-  
 306 Destructive Testing in Civil Engineering (NDTCE09), Nantes, France.
- 307 Schaeffer, K., Bearce, R., Wang, J., 2013. Dynamic modulus and damping ra-  
 308 tio measurements from free-free resonance and fixed-free resonant column  
 309 procedures. Journal of Geotechnical and Geoenvironmental Engineering  
 310 139, 2145-2155.
- 311 Seng, S., Tanaka, H., 2011. Properties of cement-treated soils during initial  
 312 curing stages. Soils and Foundations 51(5), 775-784.
- 313 Toohey, N.M., Mooney, M.A., 2012. Seismic modulus growth of lime-  
 314 stabilised soil during curing. Géotechnique 62(2), 161-170.
- 315 Verástegui Flores, R.D., Di Emidio, G., Van Impe, W.F., 2010. Small-strain  
 316 shear modulus and strength increase of cement-treated clay. Geotechnical  
 317 Testing Journal 33(1), 62-71.



1  
2  
3  
4  
5  
6  
7  
8  
9  
10  
11  
12  
13  
14  
15  
16  
17  
18  
19  
20  
21  
22  
23  
24  
25  
26  
27  
28  
29  
30  
31  
32  
33  
34  
35  
36  
37  
38  
39  
40  
41  
42  
43  
44  
45  
46  
47  
48  
49  
50  
51  
52  
53  
54  
55  
56  
57  
58  
59  
60  
61  
62  
63  
64  
65

Index	Kaolin	
Specific gravity	ASTM D 854	2.64
Liquid limit, %	ASTM D 4318	53.2
Plastic limit, %	ASTM D 4318	31.0
Swell index, ml/2g	ASTM D 5890	3.5
CEC, meq/100 g		1.38

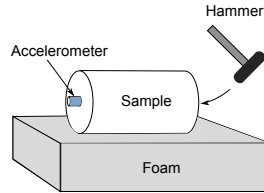
Table 1: Physical and chemical properties of Kaolin clay

Correction factor $K_E = f_L^*/f_L$			
D/L	$\nu = 0.2$	$\nu = 0.3$	$\nu = 0.4$
0.1	1.000	0.999	0.998
0.2	0.999	0.998	0.996
0.3	0.998	0.995	0.991
0.4	0.996	0.990	0.984
0.5	0.993	0.985	0.974
0.6	0.989	0.977	0.962
0.7	0.983	0.966	0.947
0.8	0.976	0.954	0.930
0.9	0.965	0.938	0.909

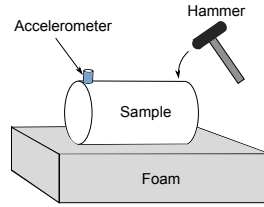
Table 2: Correction factor  $K_E$  to estimate the correct value of  $f_L$  out of the measured value  $f_L^*$

Correction factor $K_G = f_{T_r}^*/f_T$			
D/L	$\nu = 0.2$	$\nu = 0.3$	$\nu = 0.4$
0.1	0.268	0.279	0.289
0.2	0.503	0.523	0.542
0.3	0.691	0.717	0.742
0.4	0.837	0.867	0.896
0.5	0.949	0.983	1.015
0.6	1.037	1.073	1.105
0.7	1.105	1.142	1.175
0.8	1.160	1.197	1.229
0.9	1.203	1.238	1.268

Table 3: Correction factor  $K_G$  to estimate the torsional frequency  $f_T$  out of the measured transversal frequency  $f_{T_r}^*$

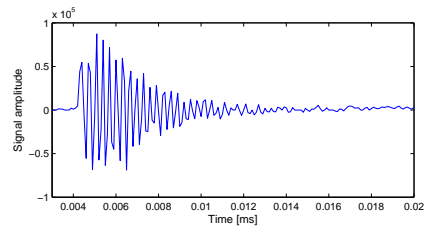


(a)

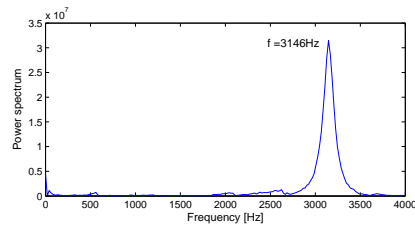


(b)

Figure 1: Free-free resonant column testing setup (a) longitudinal excitation (b) transversal excitation



(a)



(b)

Figure 2: Example of accelerometer data (a) time-domain signal (b) frequency-domain signal

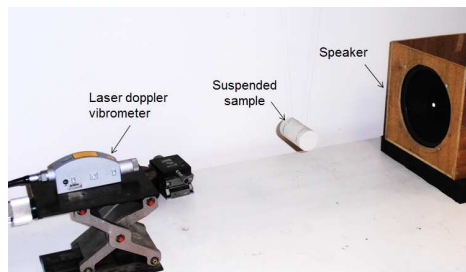


Figure 3: Laser doppler vibrometer setup

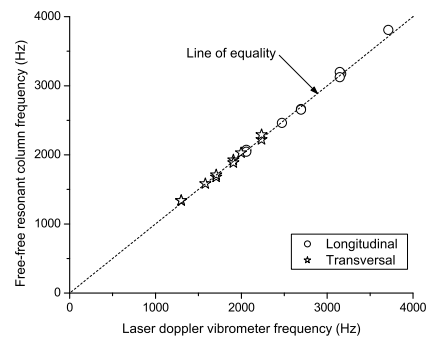
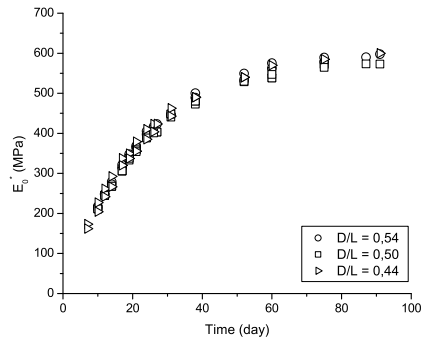
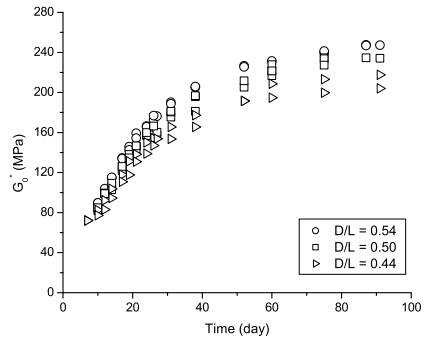


Figure 4: Correlation between measured resonant frequencies out of FFR testing and LDV

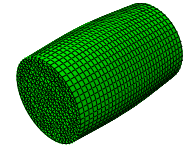


(a)

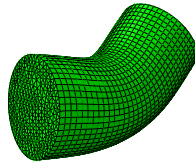


(b)

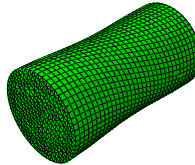
Figure 5: Estimated stiffness moduli (a) small-strain Young's modulus  $E_0$  (b) small-strain shear modulus  $G_0$



(a)



(b)



(c)

Figure 6: Vibration modes of an elastic cylindrical specimen out of modal analysis in Abaqus (a) Longitudinal (b) Transversal (c) Torsional

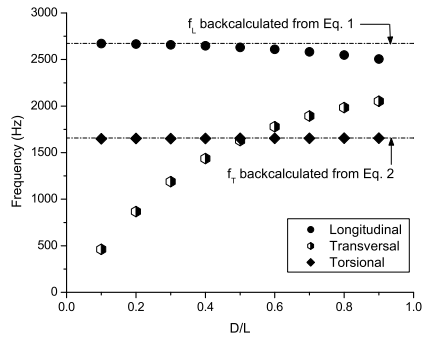
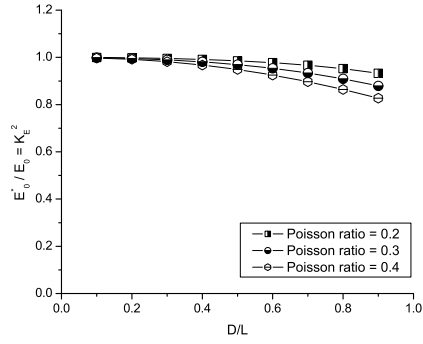
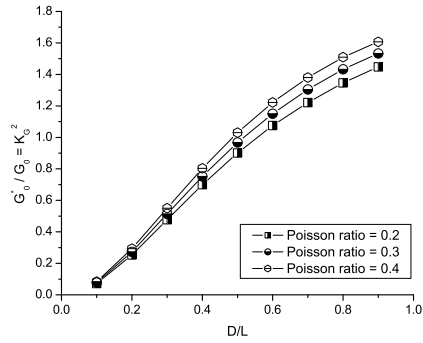


Figure 7: Longitudinal, transversal and torsional resonant frequencies of a fictitious material ( $E = 400 \text{ MPa}$ ,  $\nu = 0.3$ ,  $\rho = 1400 \text{ kg/m}^3$ ) out of Abaqus modal analysis

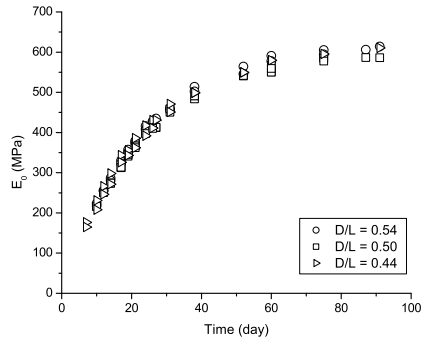


(a)

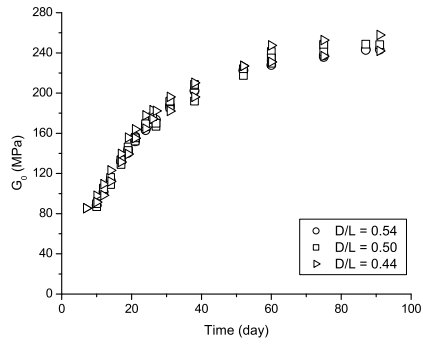


(b)

Figure 8: Correction factor to account for finite dimensions of cylindrical specimens (a) for  $E_0$  (b) for  $G_0$



(a)



(b)

Figure 9: Corrected stiffness moduli (a) small-strain Young's modulus  $E_0$  (b) small-strain shear modulus  $G_0$





To the Editorial Board of  
Soils and Foundations

Louvain-la-Neuve, June 30<sup>th</sup> 2014

Dear members of the Editorial Board,

We would like to submit our contribution for publication in the Special Issue of *Soils and Foundations* on occasion of the 6<sup>th</sup> International Symposium on Deformation Characteristics of Geomaterials, IS-Buenos Aires 2015, organized by the TC 101 (Laboratory testing) of the ISSMGE. The research paper is entitled:

*Non-destructive evaluation of stiffness moduli of cemented soil out of resonant frequency*

Authors: R.D. Verástegui Flores, G. Di Emidio, A. Bezuijen, J. Vanwalleghem, M. Kersemans

This paper summarizes the results of research aiming at evaluating the reliability of a non-destructive technique: the free-free resonant column test. It is an attractive alternative to the bender element method for the determination of small-strain stiffness of cemented and cohesive soil. The outcome of this test was compared with a superior testing method (e.g. laser doppler vibrometer) to verify its suitability. Moreover, numerical modal analysis were performed to study the impact of sample dimensions on the reliability of the interpretation formulas.

This work was not published yet nor was submitted elsewhere.

We are looking forward to hearing from you.  
Kind regards,

Daniel Verástegui Flores (corresponding author)  
Professor in Geotechnical Engineering  
Université catholique de Louvain  
Place du Levant 1 bte L5.05.01  
B-1348 Louvain-la-Neuve  
Belgium